Digital Image Analysis Method for Rapid Measurement of Rice Degree of Milling[1]

W. Liu,[2] Y. Tao,[2,3] T. J. Siebenmorgen,[2] and H. Chen[2]

ABSTRACT

Cereal Chem. 75(3):380-385

A digital image analysis method was developed to quickly and accurately measure the degree of milling (DOM) of rice. The digital image analysis method was statistically compared to a chemical analysis method for evaluating DOM, which consisted of measuring the surface lipids concentration (SLC) of milled rice. The surface lipid area percentage (SLAP) obtained by the image analysis method and the SLC obtained by chemical analysis had a high coefficient of determination using a quadratic model ($R^2 = 0.9819$) and using a logarithmic model ($R^2 = 0.9703$). The quadratic model and the logarithmic model were validated using the test data set and it received high coefficients of determination ($R^2 = 0.9502$ and $R^2 = 0.9459$, respectively).

Rice millers grade rice quality for nutritional and economic considerations and, thus, need a fast and accurate grading system as part of their milling assessment operations. The primary physical grading factors are head rice yield, which is the weight percentage of rough rice remaining as head rice (kernels that are 75% or more of their original length after milling), and degree of milling (DOM), which indicates how much bran remains on milled kernels (USDA 1979). Generally, milled rice with a high DOM level has less kernel bran than does milled rice with low DOM levels. The current methods for grading rice quality are subjective and time-consuming. This study developed a digital image analysis method that can quickly and accurately determine DOM.

DOM is an important factor in terms of the nutritional value and the economic return of the milled rice. Low DOM level rice contains more protein, vitamins, minerals, and lipids than does high DOM rice (Wadsworth et al 1991). Although low DOM level rice has greater nutritional value, it often has a lower market appeal because most consumers prefer the taste and appearance of well-milled rice. Additionally, the degree to which rice is milled inversely affects head rice yield (Sun and Siebenmorgen 1993). Therefore, adjusting DOM during the rice milling operations is essential for optimizing quality and economic return.

DOM can be measured by several methods, including visual inspection, chemical analysis, and optical measurements. Traditionally, DOM has been determined through visual inspection by trained personnel. For official grading, this judgment is made by comparing a sample to one of four official samples representing the four DOM grades (undermilled, lightly milled, reasonably well-milled, and well-milled) defined by the United States Standards for Milled Rice (USDA 1979). The closest similarity between the official representative sample and the inspection sample determines the DOM grade. Visual inspection is not only subjective but also is lacking in terms of quantitatively assessing the milling degree. For accurate measurement, more objective and quantitative methods must be employed to determine DOM.

Chemical methods of assessing DOM include the differential dye-staining procedure and the compositional analysis procedure. The differential dye-staining procedure augments the visual difference between endosperm and bran, whereas the compositional analysis method quantifies the amount of bran or bran constituents that remain on the rice kernel. Desikachar (1955), Borasio (1955), Bhattacharya and Sowbhagya (1972), and FAO (1972) used the differential dye-staining method to estimate rice DOM. Although the differential dye-staining method more readily distinguishes the difference between endosperm and bran, the assignment of DOM is still somewhat subjective because this method requires a visual assessment rather than a quantitative measurement. Barber and Benedito (1976) further evolved the differential dye-staining procedure into a quantitative procedure by defining the color bran balance (CBB) index. Milled rice kernels were soaked with a methylene blue and eosine solution in methyl alcohol, staining the bran area blue and the endosperm pink. The total bran and kernel areas were measured by planimetry. A CBB index was then assigned to indicate the DOM based on the planimetry measurements. Several other researchers attempted to determine DOM by analyzing the constituents that remained on the kernel after milling, primarily surface lipids (Autry et al 1955, Hogan and Deobald 1961, Watson et al 1975, Matthews and Spadaro 1980, Siebenmorgen and Sun 1994, Chen and Siebenmorgen 1997). However, all these chemical methods take hours to get the DOM data. Therefore, these chemical methods are too time-consuming for routine DOM measurement.

Optical measurement of DOM is contingent upon the reflection of light or the transmission of light through milled rice at selected wavelengths. Kik (1951), Stermer et al (1968), Johnson (1965), Siebenmorgen and Sun (1994), Archer and Siebenmorgen (1995) have reported the use of optical instruments for measuring DOM. Kao (1986) and Wadsworth et al (1991) developed near-infrared spectroscopy procedures to ascertain DOM. Because all these instruments utilized a bulk of rice kernels to estimate DOM, it was impossible to determine the surface lipid distribution on individual kernels. By using machine vision, each single rice kernel can be scanned completely, and DOM information can be obtained accurately through the image of each kernel.

Machine vision and image processing techniques have been widely applied throughout the agricultural and food processing fields, particularly in the quality inspection and sorting of food materials. Machine vision techniques provide a quick and objective means for measuring or evaluating the visual features of products. Researchers reported using these techniques for peach defect detection (Miller and Delwiche 1991), potato inspection (Tao et al 1990), fruit sorting (Tao 1996a,b; Tao et al 1995a,b), apple bruise detection (Upchurch et al 1994; Throop et al 1995; Tao 1996a,b; Wen and Tao 1998), corn kernel breakage classification (Liao et al 1993), corn kernel stress crack detection (Yie et al 1993), wheat classification (Zayas et al 1996, Zayas and Steele 1996), and grain classification (Shatadal et al 1995). However, there are few reports on using machine vision to measure DOM of rice. Fant et al (1994) discussed using gray-scale inten-

sity to measure DOM. Although they classified rice into the DOM grades recognized by the United States Standards for Milled Rice, they did not attempt to quantify DOM on a linear scale.

This article presents an image analysis method for quantitative measurement of the surface lipids concentration (SLC) of the milled rice kernels as an indication of DOM. The specific objectives of the research were to: 1) develop a digital image analysis system to measure the DOM (expressed quantitatively as SLC) of rice kernels, and 2) evaluate the performance of the machine vision system by correlating the results to a chemical analysis method.

MATERIALS AND METHODS

System Overview

A machine vision system using an area-scan CCD color camera was developed, as shown in Fig. 1. The color camera, equipped
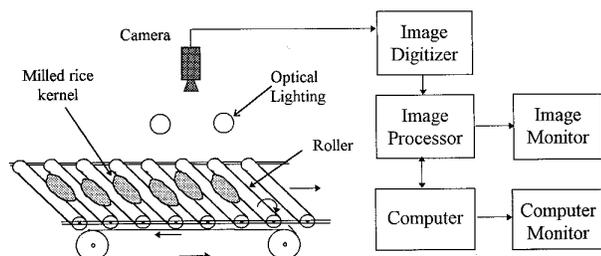

Fig. 1. Rice imaging system schematic.

with a 50-mm lens and a 40-mm C-mount lens extension tube, was mounted in an enclosure that housed a fiber optic lighting source and a rice roller conveyer. The camera was set at 101.6 mm (4 in.) above the roller conveyer, and the red channel of the camera was used to capture the images. A fiber optic lighting source (Fiber-lite high-intensity illuminator, model 180, Dolan-Jenner Industries) was used to illuminate the rice kernels. The fiber optic lighting source was set at 101.6 mm (4 in.) apart and 88.6 mm (3.5 in.) above the rice roller conveyer. The roller rotated the rice kernels to enable the camera to view each rice kernel to capture a full surface image. Two operational modes, manual rotation and motorized automatic scan, were developed for capturing the rice kernel images. Only manual rotation mode was used in this research. To reduce reflection of the ambient light, the internal surface of the enclosure and the surface of the roller were painted flat black. A personal computer with an image digitizer and image processing boards was used to collect the rice kernel images. Under the above configuration of the imaging system, the horizontal resolution of each rice kernel image was 6.998×10^{-4} in./pixel (1.775×10^{-2} mm/pixel), and the vertical resolution was 1.748×10^{-4} in./pixel (4.44×10^{-2} mm/pixel).

Surface Lipid Extraction Using Chemical Component Analysis

Surface lipids were extracted using a Soxtec System HT, which consisted of an extraction unit and a service unit (Chen et al 1997). A 5-g head rice sample was weighed into a cellulose extraction thimble and dried in a convection oven at 100°C for 1 hr. The thimble with the dried sample was then attached to magnets at the bottom of the condenser of the extraction unit. For surface extraction, the thimble was lowered to immerse the sample in 50 mL
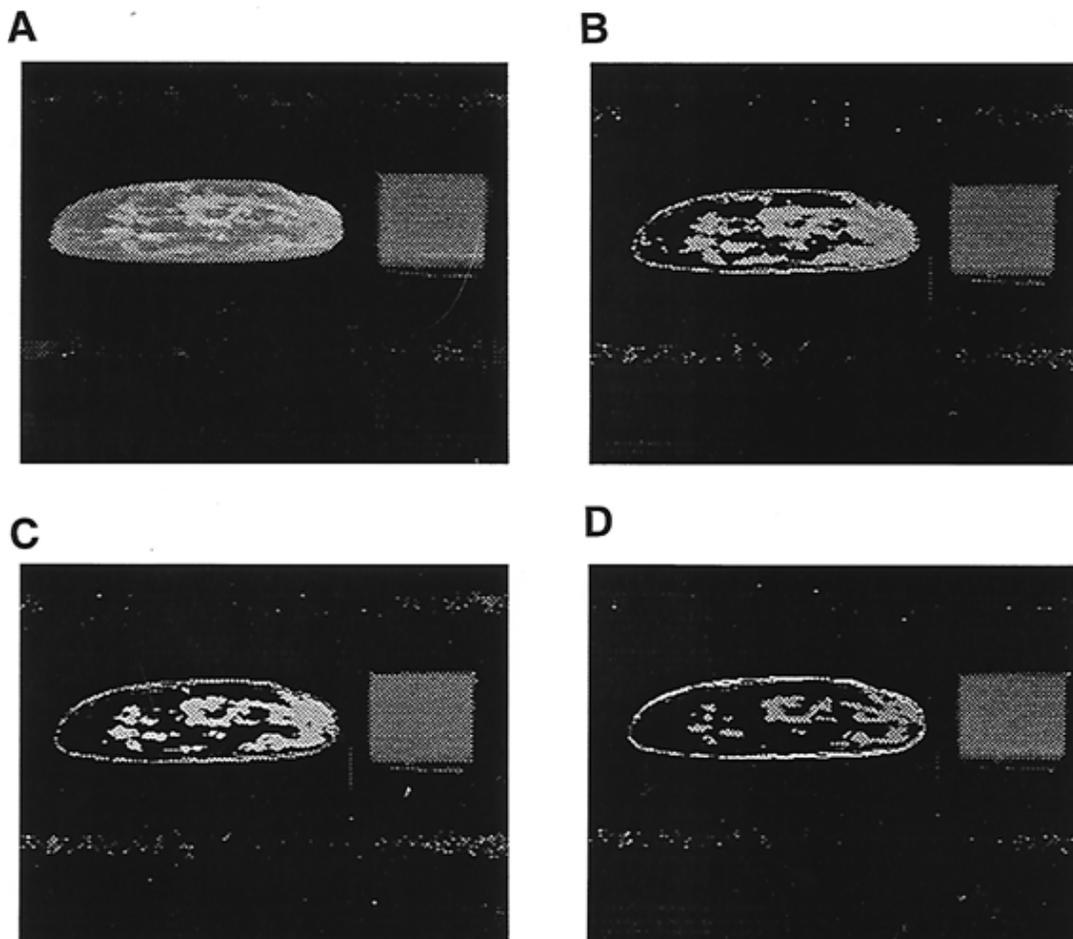

Fig. 2. Image evaluation of surface lipid concentration at three threshold T_1 values. **A,** Milled rice kernel image; **B–D,** lipid images extracted at $T_1 = 130$, 145, and 160, respectively. Rice boundary in B–D is artificially added for visual clarity. Square is a plane plastic reference material for intensity control.

of petroleum ether (boiling point 35–60°C) in an extraction cup. The solvent was evaporated by circulating around the extraction cup a hot solution (mixture of 50 mL of mineral oil with 1 L of distilled water) supplied by the service unit. The vapor was condensed into the thimble to extract most of the surface lipids from the head rice. This procedure was continued for 30 min. The thimble was then raised above the solvent surface and rinsed for another 30 min by the condensed solvent from the condenser to extract the remaining lipids on the surfaces of the kernels. After rinsing, the fluid flow through the condenser was discontinued, and the solvent from the thimble was allowed to drain for 15 min. The extraction cup was heated at 100°C for 30 min to measure dry matter, which represented the surface lipids extracted. The SLC was the weight of the surface lipids (W_{sl}) expressed as a percentage of the weight of the milled rice (W_m), which was 5 g in this experiment:

$$SLC = \frac{W_{sl}}{W_m} \times 100 \ (\%) \tag{1}$$

Surface Lipid Evaluation by Image Analysis

The SLC was also evaluated by the machine vision system. The milled rice kernel image (MRKI) was acquired by the machine vision system. Under the manual rotation mode, the MRKI of each rice kernel was obtained by combining two images representing two sides of the rice kernel. The MRKI is processed to remove the background by using a threshold $T_0 = 10$. This resulted in a binary rice image (BRI):

$$BRI(x,y) = \begin{cases} 1, & if \ MRKI(x,y) > T_0 \\ 0, & otherwise \end{cases} \tag{2}$$

where x,y are the coordinates of a pixel in the MRKI and BRI.

The whole rice surface area was measured from the BRI by counting the number of pixels in a window containing the rice kernel.

$$AREA_{whole} = \sum_{y=0}^{L-1} \sum_{x=0}^{W-1} BRI(x,y) \tag{3}$$

where L and W represented the length and the width, respectively, of the window containing the rice kernel in the BRI, and $AREA_{whole}$ is the whole rice kernel surface area.

The surface lipid image (SLI) is contingent upon the MRKI based on the threshold T_1:

$$SLI(x,y) = \begin{cases} 1, & If \ MRKI(x,y) > T_1, & T_0 < T_1 \le 255 \\ 0, & otherwise \end{cases} \tag{4}$$

The upper limit of T_1 was 255, which was determined by the 8-bit image digitizer.

The surface lipid area was calculated by summing the pixels in the window which surrounded the surface lipid area in the SLI.

$$AREA_L = \sum_{y=0}^{M-1} \sum_{x=0}^{N-1} SLI(x,y) \tag{5}$$

where the M and N represented the length and width of the window surrounding only the surface lipid area in the SLI, and $AREA_L$ is the entire surface lipid area of the rice kernel surface.

For given values of T_1, the surface lipid area percentage (SLAP) can be calculated as:

$$SLAP = \frac{AREA_L}{AREA_{whole}} \tag{6}$$

During image processing, the threshold T_0 and T_1 can be adjusted by the user for sensitivity adjustment and calibration. Examples of a raw rice kernel image and the resulting surface lipid images at three values of T_1 are shown in Fig. 2.

Samples and Experimental Procedure

The rice used for this study consisted of 17 samples of long-grain rice (Kaybonnet) with different DOM levels. All samples were selected from a single lot and milled for various durations ranging from 5 to 45 sec. Using the solvent extraction procedure described above, the SLC of each sample with two replicates was determined.

From each of the 17 samples, the image processing system was used to analyze 40 randomly selected rice kernels. These 40 kernels were separated into two groups of 20 kernels each. The first 20 from each sample were used to establish the calibration equations, and the other 20 were used to test the accuracy of the calibration equations. The front lighting was adjusted for the highest contrast between the surface lipid and endosperm. To control intensity, a plane plastic reference material 2 mm long × 2 mm wide was placed in the camera's field of view. The lighting system and the camera aperture were adjusted so that the maximum intensity level of the plastic reference material remained constant at 130 under a full intensity scale of 255. A total of 1,360 images (17 samples × 40 kernels/sample × 2 images/kernel) were collected.

TABLE I
Surface Lipid Concentration (SLC) Obtained by the Solvent Extraction Procedure and Surface Lipid Area Percentage (SLAP) Obtained by the Image Analysis Method

Sample No.	Milling Duration (sec)	SLC[a] (%)	SLAP[b] ($T_1 = 130$)	SLAP[b] ($T_1 = 145$)	SLAP[b] ($T_1 = 160$)
1	5	1.16	0.22	0.11	0.05
2	7.5	1.12	0.17	0.09	0.04
3	10	1.07	0.16	0.07	0.03
4	12.5	0.93	0.14	0.07	0.03
5	15	0.84	0.11	0.03	0.01
6	17.5	0.82	0.10	0.03	0.01
7	20	0.82	0.08	0.00	0.00
8	22.5	0.71	0.08	0.00	0.00
9	25	0.67	0.07	0.03	0.01
10	27.5	0.61	0.06	0.00	0.00
11	30	0.59	0.06	0.01	0.00
12	32.5	0.60	0.06	0.01	0.00
13	35	0.54	0.05	0.02	0.00
14	37.5	0.49	0.05	0.00	0.00
15	40	0.48	0.04	0.01	0.00
16	42.5	0.48	0.04	0.01	0.00
17	45	0.46	0.04	0.00	0.00

[a] Calculated by Eq. 1. Average of two replicates. Standard deviation ± 0.23.
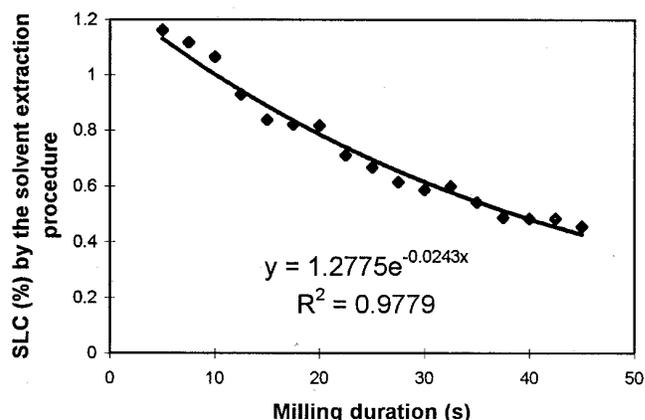[b] Calculated by Eq. 6. Average of 20 replicates. Standard deviations ± 0.05, 0.03, and 0.02, respectively.

Fig. 3. Surface lipid concentration (SLC) obtained by the solvent extraction procedure vs. milling duration, using the calibration data set.

$y = 1.2775e^{-0.0243x}$

$R^2 = 0.9779$

The rice data was analyzed using regression techniques (SAS Institute, Cary, NC). Statistical models were developed by using the REG procedure and the GLM procedure in the SAS software.

RESULTS AND DISCUSSION

Figure 2 shows a milled rice kernel image and surface lipid images extracted at three values of T_1 (130, 145, and 160). The square block is the intensity control reference material. The rice edge in the surface lipid images has been added for visual clarity. From these images, surface lipid distribution was clearly observed.

Table I shows the SLC obtained by the solvent extraction procedure and the SLAP obtained by the image analysis method for creating the calibration equation. SLC data of each sample in Table I is the average of two replicates. SLAP ($T_1 = 130$), SLAP ($T_1 = 145$), and SLAP ($T_1 = 160$) values are the average of 20 replicates of SLAP image processing results at the threshold values (T_1) of 130, 145, and 160, respectively. These values represent the calibration data set used to develop the statistical models. As the value of threshold T_1 increased, the SLAP decreased. The REG procedure in SAS suggested that the SLAP values at the threshold $T_1 = 130$ were significant at $P < 0.05$ significance level, while the SLAP values at the threshold $T_1 = 145$ and 160 were not significant at $P < 0.05$ significance level. Therefore, the SLAP values at
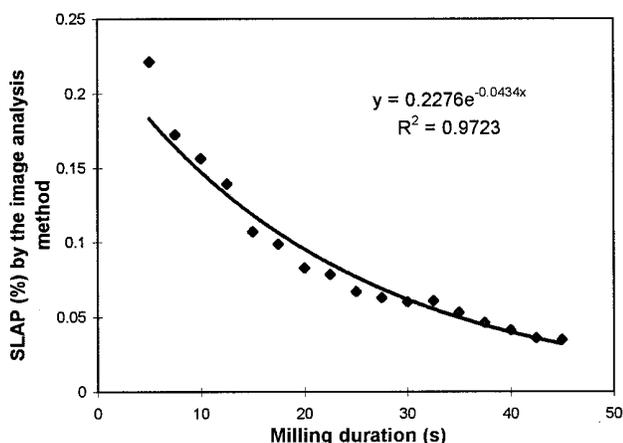
the threshold $T_1 = 130$ were used for developing calibration equations. The T_1 value <130 was not used in this study because the processed images could not represent the actual surface lipid images when the T_1 value was <130, based on the system setting.

Figure 3 shows a strong exponential relationship between SLC and milling duration as indicated by a high coefficient of determination ($R^2 = 0.9779$). Also, Fig. 4 shows a strong exponential relationship between SLAP and milling duration as indicated by a high coefficient of determination ($R^2 = 0.9723$).

Figure 5 shows the quadratic relationship between SLC obtained by the solvent extraction procedure and SLAP obtained by the image analysis method. The nonlinearity between SLC and SLAP is believed to be due to the fact that the solvent extraction procedure extracts the entire surface lipid mass, while the image analysis method indicates the amount of surface lipids by surface area. The relation between SLC and SLAP was:

$$SLC = -15.905 SLAP^2 + 7.9795 SLAP + 0.1852 \quad (7)$$

with $R^2 = 0.9819$, where SLAP value was obtained by the image analysis method at threshold $T_1 = 130$.

Fig. 4. Surface lipid area percentage (SLAP) obtained by the image analysis method at threshold $T_1 = 130$ vs. milling duration, using the calibration data set.
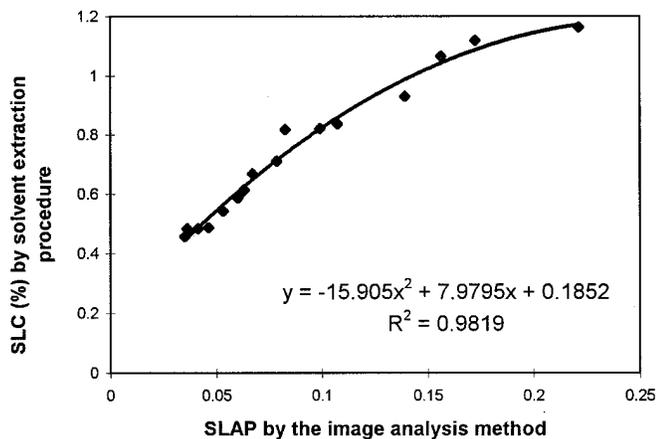

Fig. 5. Surface lipid area percentage (SLAP) obtained by the image analysis method at threshold $T_1 = 130$ vs. surface lipid concentration (SLC) obtained by the solvent extraction procedure, using the calibration data set.
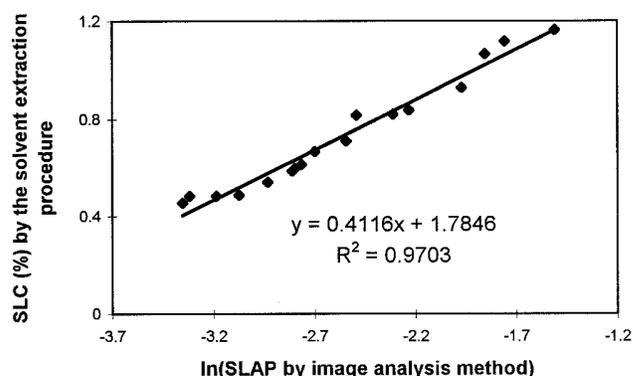

Fig. 6. Logarithmic plot of surface lipid area percentage (SLAP) obtained by the image analysis method at threshold $T_1 = 130$ vs. surface lipid concentration (SLC) obtained by the solvent extraction procedure, using the calibration data set.

TABLE II
Accuracy Analysis of Calibration Equations

Sample No.	Milling Duration (sec)	SLAP[a]	Eq. 7 Predicted SLC Value[b]	Eq. 7 Error[c]	Eq. 8 Predicted SLC Value[b]	Eq. 8 Error[c]
1	5	0.23	1.18	−0.02	1.18	−0.02
2	7.5	0.22	1.17	−0.05	1.16	−0.04
3	10	0.14	1.00	0.06	0.98	0.08
4	12.5	0.11	0.86	0.08	0.87	0.07
5	15	0.14	0.97	−0.16	0.96	−0.15
6	17.5	0.11	0.89	−0.09	0.89	−0.09
7	20	0.08	0.74	0.09	0.77	0.06
8	22.5	0.08	0.72	−0.01	0.74	−0.04
9	25	0.07	0.65	0.03	0.67	0.00
10	27.5	0.06	0.63	−0.02	0.65	−0.06
11	30	0.06	0.61	−0.03	0.63	−0.07
12	32.5	0.06	0.61	−0.02	0.63	−0.06
13	35	0.05	0.56	−0.04	0.58	−0.07
14	37.5	0.05	0.52	−0.07	0.52	−0.06
15	40	0.04	0.49	−0.01	0.47	0.02
16	42.5	0.04	0.45	0.07	0.42	0.14
17	45	0.04	0.45	0.02	0.41	0.11
Standard deviations			0.24		0.24	
Average error values				−1.03		−1.08

[a] Surface lipid area percentage calculated with Eq. 6 at threshold $T_1 = 130$ using 40 kernel images from 20 kernels of each sample.
[b] Predicted surface lipid concentration value calculated with Eq. 7 or Eq. 8.
[c] Error value obtained from Eq. 9.

Figure 6 shows the semilogarithmic plot of SLAP obtained by image analysis versus SLC obtained by the solvent extraction procedure and illustrates the linear relationship between the two methods. The resulting calibration equation is:

$$SLC = 0.4116\ln(SLAP) + 1.7846 \qquad (8)$$

with $R^2 = 0.9703$.

The high coefficients of determination ($R^2 = 0.9819$ in Fig. 5 and $R^2 = 0.9703$ in Fig. 6) indicate a significant correlation between these two analysis methods. Therefore, once the SLAP data is obtained by the image analysis method, the SLC can be predicted by either quadratic regression Eq. 7 or logarithmic regression Eq. 8. To test the accuracy of these regression equations, the validation rice group (data given in Table II) was used.

In Table II, the SLAP was obtained from the validation group by the image analysis method for testing the accuracy of the calibration equations. The SLAP data of each sample was the average of 20 replicates in the test group. The predicted SLC values were calculated by Eqs. 7 and 8, and the relative error was calculated by:

$$Error = \frac{Actual\,SLC - Predicted\,SLC}{Actual\,SLC} \qquad (9)$$

where actual SLC represents the SLC value obtained by the solvent extraction procedure in Table I.

The error values in Table II indicate the accuracy of the image analysis method. From Table II, the average errors of the predicted

SLC values of the calibration Eqs. 7 and 8 are –1.03% and –1.08%, respectively. The small average errors indicate that both calibration equations are accurate and can predict the SLC from the solvent extraction procedure if the SLAP from image analysis is given.

Figures 7 and 8 show the relationship between the actual SLC value obtained by the solvent extraction procedure and the predicted SLC value of Eqs. 7 and 8, respectively. The linear relationship in either of these figures indicates that the predicted SLC values were close to the actual SLC values. The linear relationship also shows that the calibration equation was accurate over the range of DOM levels tested.

Results obtained in this study were based on one rice variety, Kaybonnet long-grain rice. Other rice varieties and types (short- and medium-grain) should be experimented in further research.

CONCLUSION

A machine vision system was developed to evaluate rice DOM by measuring SLAP values of individual kernels. Two statistical models, a quadratic calibration equation and a logarithmic calibration equation, were obtained to predict the SLC of milled rice. The small predicted errors indicated the accuracy of both calibration equations. In contrast to the time-consuming solvent extraction procedure, the image analysis method using machine vision can quickly obtain the SLAP value of milled rice. By using the statistical model developed in this study, the SLC value from the solvent extraction procedure was easily and rapidly predicted.

Fig. 7. Predicted surface lipid concentration (SLC) using Eq. 7 based on the test data set vs. the actual SLC obtained by the solvent extraction procedure.

Fig. 8. Predicted surface lipid concentration (SLC) using Eq. 8 based on the test data set vs. the actual SLC obtained by the solvent extraction procedure.

LITERATURE CITED

Archer, T. R., and Siebenmorgen, T. J. 1995. Milling quality as affected by brown rice temperature. Cereal Chem. 72:304-307.

Autry, H. S., Grigorief, W. W., Altschul, A. M., and Hogon, J. T. 1955. Effects of milling conditions on the breakage of rice grains. J. Agric. Food Chem. 3:593-599.

Barber, S., and Benedito de Barber, C. 1976. An approach to the objective measurement of the degree of milling. Rice Process Eng. Center 2(2):1-8.

Bhattacharya, D. R., and Sowbhagya, C. M. 1972. A colorimetric bran pigment method for determining the degree of milling rice. J. Sci. Food Agric. 23:161-169.

Borasio, L. 1955. Macrocolorimetric method for evaluation of the final product of rice processing. Ann. Stn. Sper. Risicolture Colture Irrigue. 3:51-56.

Chen, H. and T. J. Siebenmorgen. 1997. Effect of rice kernel thickness on degree of milling and associated optical measurements. Cereal Chem. 74:821-825.

Chen, H., Marks, B. P., and Siebenmorgen, T. J. 1997. Quantifying surface lipid content of milled rice via visible/near-infrared spectroscopy. Cereal Chem. 74:826-831.

Desikachar, H. S. R. 1955. Determination of the degree of polishing in rice. I. Some methods for comparison of the degree of milling. Cereal Chem. 32:71-77.

Fant, E., Casady, W., and Goh, D. 1994. Grey-scale intensity as a potential measurement for degree of rice milling. J. Agric. Eng. Res. 58:89-97.

FAO. 1972. Degree of milling of rice: The standard method adopted by the food agency, government of Japan. Sub-Group on Rice Grading and Standardization. Intergovernmental Group of Rice, Rome, May 10-12, 1972. FOA Document CCP: RI/CS C.R.S. 1. FAO: Rome.

Hogan, J. T., and Deobald. H. J. 1961. Note on the method of determining the degree of milling of whole milled rice. Cereal Chem. 38:291-293.

Johnson, R. M. 1965. Light-reflectance meter measures degree of milling and parboiling of parboiled rice. Cereal Chem. 42:167-174.

Kao, C. 1986. Determination of rice milling degree with near infrared reflectance method. Page 101 in: Proc. 21st Rice Technical Working Group.

Kik, M.C. 1951. Determining degree of milling by photoelectric means. Rice J. 54(12):18-22.

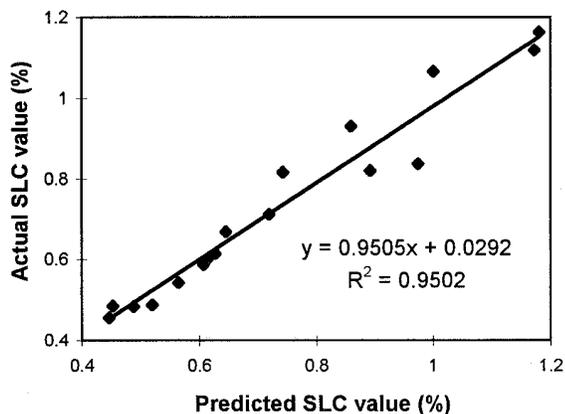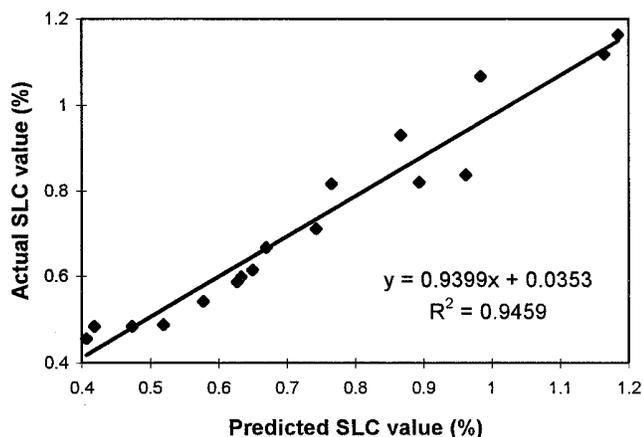Liao, K., Paulsen, M. R., Reid, J. F., Ni, B. C., and Bonifacio-Maghirang,

E. B. 1993. Corn kernel breakage classification by machine vision using a neural network classifier. Trans. ASAE 36:1949-1953.

Matthews, J., and Spadaro, J. J. 1980. Milling degrees of Starbonnet brown assayed. Rice J. 83:12-19.

Miller, B. K., and Delwiche, M. J. 1991. Peach defect detection with machine vision. Trans. ASAE 34:2588-2597.

Shatadal, P., Jayas, D. S., and Bulley, N. R. 1995. Digital image analysis for software separation and classification of touching grains. II. Classification. Trans. ASAE 38:645-649.

Siebenmorgen, T. J., and Sun, H. 1994. Relationship between milled rice surface fat concentration and degree of milling as measured with a commercial milling meter. Cereal Chem. 71:327-329.

Stermer, R. A. 1968. An instrument for objective measurement of degree of milling and color of milled rice. Cereal Chem. 45:358-364.

Sun, H., and Siebenmorgen, T. J. 1993. Milling characteristics of various rough rice kernel thickness fractions. Cereal Chem. 70:727-733.

Tao, Y. 1996a. Methods and apparatus for sorting objects including stable color transformation. U.S. patent 5,533,628.

Tao, Y. 1996b. Spherical transform of fruit images for on-line defect extraction of mass objects. Optical Eng. 35:344-350.

Tao, Y., Morrow, C. T., Heinemann, P. H., and Sommer, J. H. 1990. Automated machine vision inspection of potatoes. Paper 90-3531. ASAE: St. Joseph, MI.

Tao, Y., Chance, L. and Liu, B. 1995a. Full scale machine vision sorting system design—Factors and considerations. In: Food Processing Automation. ASAE. 3:14-22.

Tao, Y., Morrow, C. T., Heinemann, P., Sommer, H. J., III. 1995b.

Fourier-based separation technique for shape grading of potatoes using machine vision. Trans. ASAE. 38:949-957.

Throop, J. A., Aneshansley, D. J., and Upchurch, B. L. 1995. An image processing algorithm to find new and old bruises. Appl. Eng. Agric. 11:751-757.

Upchurch, B. L., Throop, J. A., and Aneshansley, D. J. 1994. Influence of time, bruise-type, and severity on near-infrared reflectance from apple surfaces for automatic bruise detection. Trans. ASAE. 37:1571-1575.

USDA. 1979. Inspection handbook for the sampling, inspection, grading and certification of rice. HB 918-11. USDA: Washington, DC.

Wadsworth, J. I., Sequeira, D. J., Velupillai, L., and Verma, L. R. 1991. Rice degree of milling measured by NIR. Paper 91-6030. ASAE: St. Joseph, MI.

Watson, C. A., Dikeman, E., and Stermer, R. A. 1975. A note on surface lipid content and scanning electron microscopy of milled rice as related to degree of milling. Cereal Chem. 52:742-747.

Wen, Z., and Tao, Y. 1998. Fuzzy-based determination of model and parameters of dual-wavelength vision system for on-line apple sorting. Optical Eng. 37:293-299

Yie, T. J., Liao, K., Paulsen, M. R., Reid, J. F., and Maghirang, E. B. 1993. Corn kernel stress crack detection by machine vision. Paper 93-3526. ASAE: St. Joseph, MI.

Zayas, I. Y., and Steele, J. L. 1996. Image texture analysis for discrimination of mill fractions of hard and soft wheat. Cereal Chem. 73:136-142.

Zayas, I. Y., Martin, C. R., Steele, J. L., and Katsevich, A. 1996. Wheat classification using image analysis and crush-force parameters. Trans. ASAE 39:2199-2204.